

## Shear-type Modulated Structure of $\text{Bi}_{2.49}\text{Sr}_{2.00}\text{Co}_{2.22}\text{O}_x$

K. Yubuta\*, S. Begum<sup>1</sup>, Y. Ono<sup>1</sup>, Y. Miyazaki<sup>1</sup> and T. Kajitani<sup>1</sup>

Institute for Materials Research, Tohoku Univ., Sendai 980-8577, Japan

\* corresponding author, e-mail: yubuta@imr.tohoku.ac.jp

<sup>1</sup>Graduate School of Engineering, Tohoku Univ., Sendai 980-8579, Japan

The modulated structure of  $\text{Bi}_{2.49}\text{Sr}_{2.00}\text{Co}_{2.22}\text{O}_x$  is studied by means of the electron diffraction measurements and high-resolution electron microscopy. The crystal structure consists of two interpenetrating subsystems of a  $\text{CoO}_2$  (CdI<sub>2</sub>-type triangular lattice) sheet and a distorted four-layered  $\text{Bi}_2\text{Sr}_2\text{O}_4$  rock-salt-type block. Both subsystems have common  $a$ -,  $c$ -axes and  $\beta$ -angle with  $a = 4.99 \text{ \AA}$ ,  $c = 15.25 \text{ \AA}$  and  $\beta = 93.6^\circ$ . On the other hand, the crystal structure is incommensurately modulated parallel to the  $b$ -axis, among which  $b_1 = 2.78 \text{ \AA}$  for the  $\text{CoO}_2$  sheet and  $b_2 = 5.12 \text{ \AA}$  for the  $\text{Bi}_2\text{Sr}_2\text{O}_4$  rock-salt-type block, respectively. The misfit ratio,  $b_1/b_2 \sim 0.54$ , characterizes the structural analogue as  $[\text{Bi}_{2.08}\text{Sr}_{1.67}\text{O}_y]_{0.54}[\text{CoO}_2]$ . This compound has some varieties of modulation vectors,  $q_1 = -a^* + 0.54b_1^*$ ,  $q_2 = 0.05b_1^*$  and locally  $q_3 = -0.14a^* + 0.10b_1^*$ . The intrinsic modulation vector  $q_2$  is different from the one in  $[\text{Bi}_{0.87}\text{SrO}_2]_2[\text{CoO}_2]_{1.82}$  studied by Leligny *et al.* High-resolution images taken with the incident electron beam parallel to the  $a$ - and  $c$ -axes clearly exhibit modulated atomic arrangements. The local modulation mode characterized by the vector  $q_3$  is related to the shear deformation in  $a$ - $b$  plane. It is natural to assume that the observed stripe pattern is a sign of a relaxation mechanism of the strain.

Key words: thermoelectric compound, electron diffraction, high-resolution image, shear structure, residual stress

### 1. INTRODUCTION

The cobalt oxides Bi-Sr-Co-O have been synthesized as promising thermoelectric materials [1-3]. In addition, the Bi-Sr-Co-O crystals are regarded as a representative compound of the misfit-layered crystals. It has been found that the compound consists of edge-sharing triangular  $\text{CoO}_2$  sheets and four-layered  $\text{Bi}_2\text{Sr}_2\text{O}_4$  rock-salt-type block layers interpenetrating alternately in the  $c$ -axis direction by Leligny *et al.* [4,5]. These two subsystems make up an incommensurate superlattice along the  $b$ -axis.

Recently, we have studied the structure of new layered Rh-oxides  $[\text{Bi}_{1.79}\text{Sr}_{1.98}\text{O}_y]_{0.63}[\text{RhO}_2]$  [6] and  $[\text{Bi}_{1.94}\text{Ba}_{1.83}\text{O}_y]_{0.56}[\text{RhO}_2]$  [7] by means of transmission electron microscopy. In Ba-Rh system, two dimensional modulation was observed in  $a$ - $b$  plane as in  $[\text{Bi}_2\text{Ba}_{1.8}\text{Co}_{0.2}\text{O}_4]^{\text{RS}}[\text{CoO}_2]_2$  [8], but such modulation was not observed in  $[\text{Bi}_{0.87}\text{SrO}_2]_2[\text{CoO}_2]_{1.82}$  [5].

Begum *et al.* have studied phase stability of the Bi-Sr-Co-O ceramics near the Bi : Sr : Co = 2 : 2 : 2 (Bi-222) composition and obtained single phase samples at the nominal compositions of Bi : Sr : Co = 2 : 1.9 : 2.1 (sample A) [9]. Samples A exhibit metallic behavior in the temperature range from 77 °C to 700 °C and Seebeck coefficient increases with increasing temperature. The thermal conductivity was found to be nearly temperature-independent at temperatures between 77 °C and 327 °C ( $=0.9 \text{ Wm}^{-1}\text{K}^{-1}$ ).

To understand the physical properties, it is necessary to know the detailed crystal structures. Present study was pursued for the modulated structure analysis by means of the electron diffraction measurements and high-resolution electron microscopy.

### 2. EXPERIMENTAL

Polycrystalline samples were prepared by the standard solid-state reaction method. A mixture of  $\text{Bi}_2\text{O}_3$ ,  $\text{SrCO}_3$  and  $\text{Co}_3\text{O}_4$  powder weighed in the molar ratio at Bi : Sr : Co = 2 : 1.9 : 2.1 (sample A in ref. [9]) was mixed in an agate mortar and pressed into pellets. The pellets were heated at 800 °C for 12 h in air. Then, the samples were furnace-cooled to room temperature. After grinding, the powders were re-pelletized and heated at 840 °C for 12 h in air followed by the furnace-cooling.

Chemical analysis was carried out using an electron probe microanalyzer (EPMA:JEOL JXA-8621MX). An averaged composition ratio was obtained from more than five different sample positions, being expressed as Bi : Sr : Co = 2.49 : 2.00 : 2.22. It was notice that Bi-content was richer than that of Sr.

TEM specimens were prepared by mechanical polishing and ion milling.

Electron diffraction patterns and high-resolution electron microscopy images were obtained using a 200 kV electron microscope (JEM-2010) at a resolution of 1.9 Å.

### 3. RESULTS AND DISCUSSION

#### 3.1 Electron diffraction patterns and HREM images

Figs. 1(a)-1(d) show the electron diffraction patterns of  $\text{Bi}_{2.49}\text{Sr}_{2.00}\text{Co}_{2.22}\text{O}_x$  taken with the incident beam parallel to the four principal axes. On the basis of obtained diffraction patterns, it was found that the present crystal has a composite structure consisting of two monoclinic subsystems, which have common  $a$ - and  $c$ -axes and mutually incommensurate  $b_1$ - and  $b_2$ -axes.

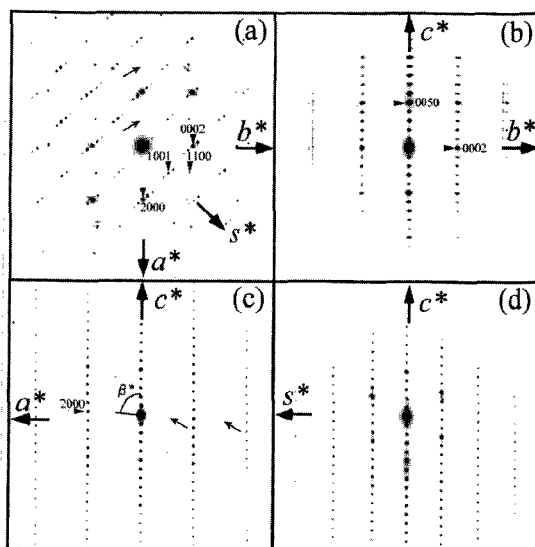


Fig. 1 Electron diffraction patterns of  $[\text{Bi}_{2.08}\text{Sr}_{1.67}\text{O}_y]_{0.54}[\text{CoO}_2]$ , taken with the incident electron beam parallel to (a)  $[0010]$ , (b)  $[1000]$ , (c)  $[0101]$  and (d)  $[100-1]$ .

Four axis lengths and  $\beta$ -angles were thus estimated as  $a = 4.99 \text{ \AA}$ ,  $b_1 = 2.78 \text{ \AA}$  ( $\text{CdI}_2$ -type sheets),  $b_2 = 5.16 \text{ \AA}$  (rock-salt-type blocks),  $c = 15.25 \text{ \AA}$  and  $\beta = 93.6^\circ$ . The ratio of  $b_1/b_2 \sim 0.54$  gives the structural analogue as  $[\text{Bi}_{2.08}\text{Sr}_{1.67}\text{O}_y]_{0.54}[\text{CoO}_2]$ .

On the basis of the systematic absence of reciprocal lattice points, possible space groups of the two subsystems are  $P2_1$  or  $P2_1/m$ -types. We assume centrosymmetric  $P2_1/m$ -type unit cells, having the highest symmetry among them. It is exhibited that this symmetry is not identical with that of  $[\text{Bi}_{0.87}\text{SrO}_2]_2[\text{CoO}_2]_{1.82}$  [5], since the reflection conditions shown in Figs. 1(c) and 1(d) are different.

Characteristic feature of the diffraction pattern in Fig. 1(a) is the streaks, continuous reflection lines, shown parallel to  $[100-1]^*$ , as similarly observed in  $\text{Bi}_2\text{M}_3\text{Co}_2\text{O}_y$  ( $M = \text{Sr}, \text{Ba}$ ) [10],  $\text{Bi}_{2-x}\text{Pb}_x\text{Sr}_2\text{Co}_2\text{O}_y$  [3],  $[\text{Bi}_2\text{Ba}_{1.8}\text{Co}_{0.2}\text{O}_4]^{\text{RS}}[\text{CoO}_2]_2$  [8] and  $[\text{Bi}_{1.94}\text{Ba}_{1.83}\text{O}_y]_{0.56}[\text{RhO}_2]$  [7]. Hervieu *et al.* concluded that they are generated by an intrinsic modulation of  $[\text{Bi}_2\text{Ba}_{1.8}\text{Co}_{0.2}\text{O}_4]$  block [8]. By means of HREM imaging technique, we have directly observed that the  $[\text{Bi}_{1.94}\text{Ba}_{1.83}\text{O}_y]_{0.56}[\text{RhO}_2]$  compound has a shear-type modulation in the  $a$ - $b$  plane. On the other hand, such reflection line was not observed in  $[\text{Bi}_{0.87}\text{SrO}_2]_2[\text{CoO}_2]_{1.82}$  [5], which is Bi-poor relative to Sr.

There are satellite reflections in Figs. 1(a) and 1(b), but no satellite reflection is seen in Figs. 1(c) and 1(d). Figs. 2(a) and 2(b) show enlarged patterns of parts of Figs. 1(a) and 1(b), respectively. There are three modulation vectors  $q_1$ ,  $q_2$  and  $q_3$  in Figs. 2. In Fig. 2(b), satellite reflections are observed only in the vicinity of the fundamental reflections. The origin of the vectors  $q_1$  is the difference in the two  $b$ -axis lengths of the two subsystems but  $q_2$  is due to the intrinsic modulation in the rock-salt block. Modulation vectors can be expressed as  $q_1 = -a^* + 0.54b_1^*$  and  $q_2 = 0.05b_1^*$ , respectively.

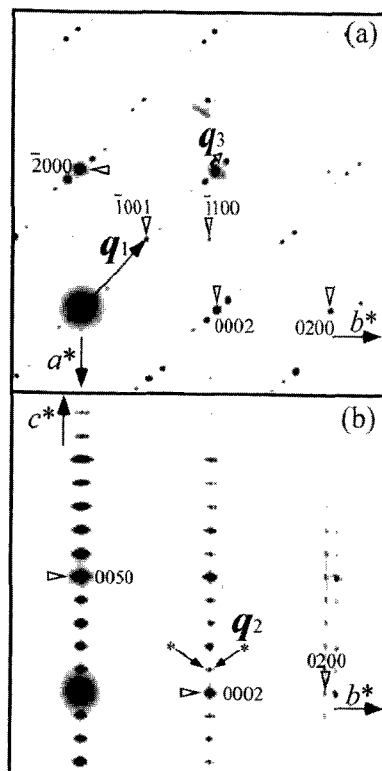


Fig. 2 Enlarged electron diffraction patterns (a) and (b) of parts of Fig. 1(a) and (b), respectively.

In  $[\text{Bi}_{0.87}\text{SrO}_2]_2[\text{CoO}_2]_{1.82}$  [5], an intrinsic modulation vector was  $q_{11} = 0.293 a^* + 0.915 c^*$  being incommensurate either in  $a^*$ - and  $c^*$ -axes. This difference could be due partly to the significant difference in the Bi/Sr ratio, being 1.25 in  $[\text{Bi}_{2.08}\text{Sr}_{1.67}\text{O}_y]_{0.54}[\text{CoO}_2]$  and 0.93 in  $[\text{Bi}_{0.87}\text{SrO}_2]_2[\text{CoO}_2]_{1.82}$ , respectively. Compared with present  $q_2$  of the title compound, there are two important characteristics. The first point is that  $q_2$  is only clearly seen in the  $b^*$ - $c^*$  plane in  $[\text{Bi}_{2.08}\text{Sr}_{1.67}\text{O}_y]_{0.54}[\text{CoO}_2]$ , while  $q_{11}$  exists on  $a^*$ - $c^*$  plane in the  $[\text{Bi}_{0.87}\text{SrO}_2]_2[\text{CoO}_2]_{1.82}$ , respectively. The second point is that the  $c^*$  component of  $q_2$  is zero in the present  $[\text{Bi}_{2.08}\text{Sr}_{1.67}\text{O}_y]_{0.54}[\text{CoO}_2]$ .

Figs. 3(a) and 3(b) represent the filtered high-resolution images, corresponding to Figs. 1(a) and 1(b) and were obtained by inverse Fourier synthesis, using (a)  $hk0m$  reflections with satellite ones, (b)  $0klm$  ones with satellite ones, respectively.

Characteristic shear type discontinuity lines, for which one can notice that the shear displacement is not sine-wave-type, are clearly observed at the positions indicated by arrowheads in Fig. 3(a). These discontinuity lines correspond to the structural modulation mode characterized by the vector,  $q_3 = -0.14a^* + 0.10b_1^*$ . In the stripe ranges seen between two discontinuity lines, the image contrast is slightly bright and disturbed. The atomic arrangement projected to  $[1001]$  direction seems perfect but the atomic arrangements in  $[-1001]$  direction are very disturbed.

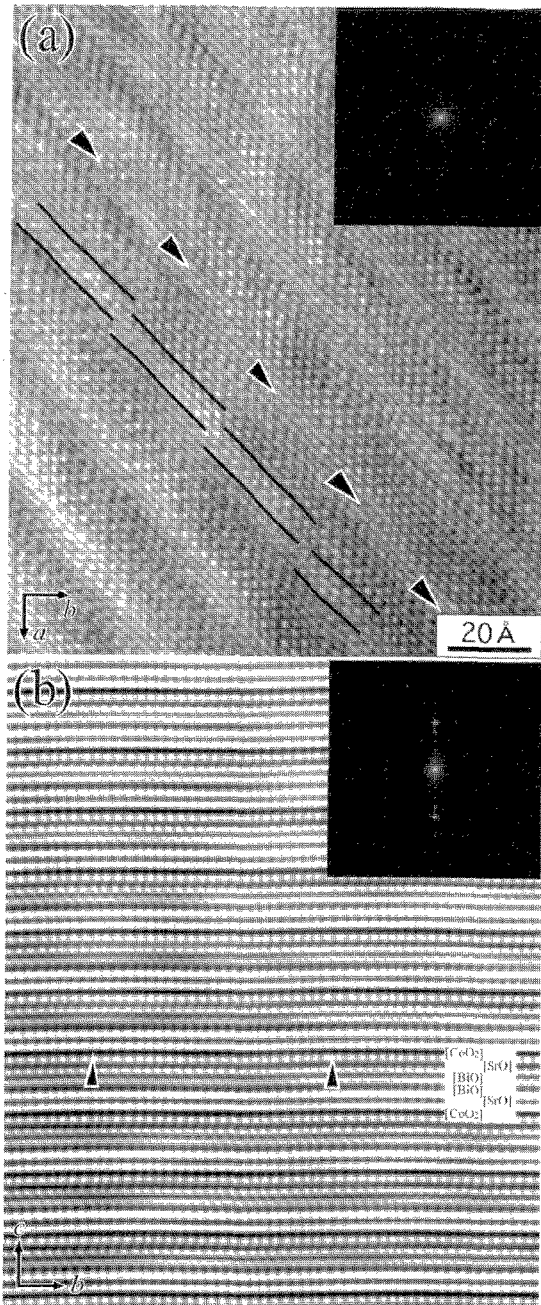


Fig. 3 Fourier-filtered high-resolution image taken with the incident electron beam parallel to (a) [0010], (b) [1000]. The insets show the power spectra of observed images.

It is also conceivable that the structural modulations in  $a$ - $b$  plane are due to a structural and concentration alterations in the  $\text{Bi}_2\text{Sr}_2\text{O}_4$  rock-salt-type blocks being similar to a case of  $[\text{Bi}_2\text{Ba}_{1.8}\text{Co}_{0.2}\text{O}_4]^{\text{KS}}[\text{CoO}_2]_2$ . In the present compound, deficiency at the Sr-site and the concentration difference between  $\text{Bi}^{3+}$  and  $\text{Sr}^{2+}$  ions are obviously large. Since the ionic radii of  $\text{Bi}^{3+}$ ,  $r_{\text{S-P}} = 0.99$  Å, and  $\text{Sr}^{2+}$ ,  $r_{\text{S-P}} = 1.16$  Å, are different, above modulation modes could be originated from a chemical ordering of  $\text{Bi}^{3+}$  and  $\text{Sr}^{2+}$  ions. It is noticed that there exists contrast modulation in Fig. 3(b). The arrowheads exhibit the long periodicity, at about 55 Å,

corresponding to the modulation vector  $q_2$ .

### 3.2 Shear deformation and Residual strains

As indicated in filtered images, it is found that  $\text{CdI}_2$ -type layers and rock-salt-type blocks are mutually strained, nearly two dimensionally, i.e.  $e_{11} = -e_{22}$  where  $e_{ij}$  is the strain tensor element. It is pointed out that the averaged values of  $a$ - and  $b_2$ -axis lengths are nearly equal to the natural  $M$ - $O$ - $M$  bond length, which is expected from the ionic radii. Those lengths are, respectively, 5.415 Å and 5.42 Å in Ba-Rh compound, 5.08 Å and 5.02 Å in Sr-Rh compound and 5.075 Å and 5.02 Å in this crystal.

$\text{Bi-M-Rh-O}$  system, in which  $M = \text{Ba}$  or  $\text{Sr}$ , is a typical misfit layered one which has  $\text{Bi-O}$  double layers as in the present system. There is significant difference in the residual strain of rock-salt-type blocks, i.e.  $e_{11} = -e_{22} = -0.0065$  in Ba-Rh system,  $e_{11} = -e_{22} = +0.0394$  in Sr-Rh system and  $e_{11} = -e_{22} = -0.0167$  in the present system. That is, the rock-salt layers are compressed along the  $a$ -axis and expanded along the  $b_2$ -axis, as shown in Fig. 4(a). Although  $a$ -axis length,  $a = 4.99$  Å, is longer than that of Ca349 phase [11], 4.83 Å, and  $[\text{Bi}_{0.87}\text{SrO}_2]_2[\text{CoO}_2]_{1.82}$  [5], 4.90 Å,  $a$ -axis length is not long enough to release the compressive stress for the rock-salt blocks, since the natural bond length is in the range of 5.02 Å to 5.075 Å. In  $\text{CdI}_2$ -type layers, on the other hand, the tensile stress along the  $a$ -direction and the compressive one along the  $b_1$ -direction are simultaneously resided, respectively, as shown in Fig. 4(b). It is consistent with the fact that  $b_1$ -length of this crystal,  $b_1 = 2.78$  Å, is shorter than those of Ca349 phase with  $b_1 = 2.82$  Å and  $[\text{Bi}_{0.87}\text{SrO}_2]_2[\text{CoO}_2]_{1.82}$  with  $b_1 = 2.81$  Å. It is, thus, suggested that the two dimensional strains are resided either in the rock-salt-type blocks as well as  $\text{CdI}_2$  layers in the present system. It is natural to assume that the observed stripe pattern in Fig. 3(a) is a sign of a relaxation mechanism of the strain. Similarly, the compounds  $[\text{Bi}_2\text{Ba}_{1.8}\text{Co}_{0.2}\text{O}_4]^{\text{RS}}[\text{CoO}_2]_2$  and  $[\text{Bi}_{1.94}\text{Ba}_{1.83}\text{O}_y]_{0.56}[\text{RhO}_2]_2$ , which have a shear-type modulation parallel to  $[100-1]^*$  direction in the  $a^*-b^*$  plane, are distorted in (a) and (b)-types.

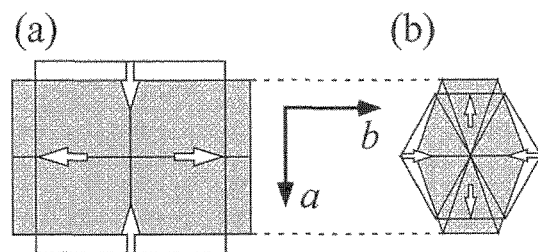


Fig. 4 Schematic representation of  $a$ - $b$  real lattice planes. The distortion-types of (a) the rock-salt-blocks and (b) the hexagonal  $\text{CdI}_2$ -type layers. Arrows with black edge show the direction of the residual strain.

The shear-type structural deformation causes local discontinuity, i.e., a kind of discommensuration in the  $a$ - $b$  plane. Such deformation is frequently recognized in martensitic transformation by which slipping, buckling and twinning deformation mode are frequently seen in the directions at about 45 degree from the compressive

or tensile stress. It is conceivable that the observed discontinuity contrasts in the title compound correspond to a pre-stage of the sliding deformation (Fig. 5).

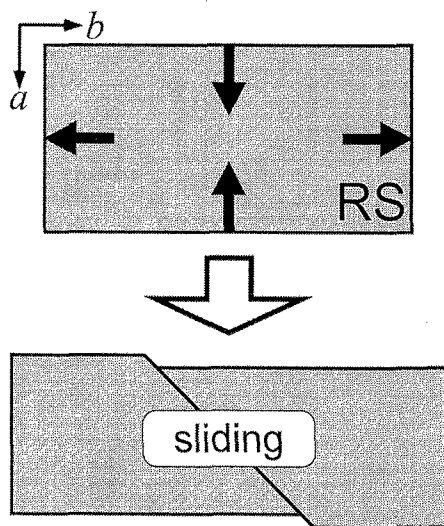


Fig. 5 Schematic illustration of the pre-stage of sliding deformation in  $a$ - $b$  real lattice planes.

It is well known that the superconducting oxide  $\text{Bi2122}$  has intrinsic corrugation deformation due to the misfit between the  $[\text{Bi}_2\text{O}_{2+\delta}]$  plus  $(\text{Sr}_2\text{O}_2\text{Ca})$  layers and double pyramidal  $\text{Cu-O}_5$  layers [12]. Similarly, the corrugation deformation exists in this thermoelectric compound.

#### 4. CONCLUSION

We have studied the modulated structure of  $\text{Bi}_{2.49}\text{Sr}_{2.00}\text{Co}_{2.22}\text{O}_x$ . This compound has a misfit-layered structure, for which the chemical formula is  $[\text{Bi}_{2.08}\text{Sr}_{1.67}\text{O}_y]_{0.54}[\text{CoO}_2]$ . This crystal has two modulation vectors,  $q_1 = -a^* + 0.54b_1^*$  and  $q_2 = 0.05b_1^*$ . An additional modulation vector,  $q_3 = -0.14a^* + 0.10b_1^*$ , is also observed locally. Curving and fluctuating features of two subsystems are directly observed along  $a$ - and  $c$ -axes, respectively. In the  $a$ - $b$  plane, a shear-type modulation is also locally found. An important point to emphasize is that this compound has displacive and concentration modulations plus semi-periodic discommensuration-type shear deformations.

#### ACKNOWLEDGMENTS

This study was partly supported by the Core Research for Evolution Science and Technology (CREST) Project of Japan Science and Technology Agency (JST) and also by a Grant-in-Aid for Scientific Research from the Ministry of Education, Culture, Sports, Science and Technology of Japan.

#### REFERENCES

- [1] R. Funahashi, I. Matsubara and S. Sodeoka, *Appl. Phys. Lett.*, **76**, 2385 (2000).
- [2] T. Itoh and I. Terasaki, *Jpn. J. Appl. Phys.*, **39**, 6658 (2000).
- [3] T. Yamamoto, I. Tsukada, K. Uchinokura, M. Takagi, T. Tsubone, M. Ichihara and K. Kobayashi, *Jpn. J. Appl. Phys.*, **39**, L747 (2000).

*Phys.*, **39**, L747 (2000).

[4] H. Leligny, D. Grebille, O. Pérez, A. C. Masset, M. Hervieu, C. Michel and B. Raveau, *C. R. Acad. Sci. Paris Série IIC*, **2**, 409 (1999).

[5] H. Leligny, D. Grebille, O. Pérez, A. C. Masset, M. Hervieu and B. Raveau, *Acta Cryst. B* **56**, 173 (2000).

[6] K. Yubuta, S. Okada, Y. Miyazaki, I. Terasaki and T. Kajitani, *Jpn. J. Appl. Phys.*, in press.

[7] K. Yubuta, S. Okada, Y. Miyazaki, I. Terasaki and T. Kajitani, *Jpn. J. Appl. Phys.*, in press.

[8] M. Hervieu, A. Maignan, C. Michel, V. Hardy, N. Créon and B. Raveau, *Phys. Rev. B* **67**, 045112 (2003).

[9] S. Begum, Y. Ono, Y. Miyazaki and T. Kajitani, *Trans. Mat. Res. Soc. Jpn.*, **30**, 495 (2005).

[10] J.-M. Tarascon, R. Ramesh, P. Barboux, M. S. Hedge, G. W. Hull, L. H. Greene, M. Giroud, Y. LePage, W. R. McKinnon, J. V. Waszcek and L. F. Schneemeyer, *Solid State Comm.*, **71**, 663 (1989).

[11] Y. Miyazaki, M. Onoda, T. Oku, M. Kikuchi, Y. Ishi, Y. Ono, Y. Morii and T. Kajitani, *J. Phys. Soc. Jpn.*, **71**, 491 (2002).

[12] N. L. Saini and A. Bianconi, *Int. J. Modern Phys. B* **14**, 3649 (2000).

(Received December 11, 2005; Accepted March 31, 2006)